

### 3D NUMERICAL ANALYSIS AND STRUCTURES FORMATION IN ACCRETING WHITE DWARFS

DANIELA BONEVA<sup>1</sup>, LACHEZAR FILIPOV<sup>2</sup>, DEYAN GOTCHEV

*Space Research and Technology Institute – Bulgarian Academy of Sciences*

**Abstract.** The majority of accreting white dwarfs are dynamically bounded with a companion in a binary star configuration. We aim to examine structure's properties of the flow in accreting zone, surrounding the white dwarf star. We consider a gas-dynamical system that allows 3D modeling of physical processes in the close components. Multi-physics, multi-algorithm, adaptive numerical code is applied. The methods implied are both suitable for time-dependent, implicit computations and consist of a hydrodynamical module in their architectures. The results reveal the pattern formation character and dynamics of interaction in the binary star's flow. A density distribution model through the whole disc's structure is suggested.

#### 1. INTRODUCTION

Binary systems in which a white dwarf accretes from a close companion star are quite common in the Galaxy. The importance of their study comes from the fact that they provide an opportunity to examine the accretion process in isolation, since other sources of luminosity, in particular the companion star, are relatively unimportant. When nuclear burning does occur on the surface of a white dwarf, it is likely that the reaction tends to produce a great brightness but short duration (Frank et al. 2002). For almost whole of its last lifetime no nuclear burning occurs, and the white dwarf may derive its entire luminosity from accretion. A critical stage in the evolution of a compact WD binary is the period just after mass transfer has been initiated (Dan et al. 2012). For the binary to survive, the mass transfer must be stable, which depends sensitively on the internal structure of the donor star, the binary mass ratio, and the angular momentum transport mechanisms (e.g. Marsh et al. 2004; Gokhale et al. 2007). In astrophysics, the problems of structures development have been investigated mainly numerically (e.g. Lithwick 2009, Godon and Livio 1999). In the papers of Shen et al. (2006) and Barranco and Marcus (2005), 2D compressible simulations and “inelastic code” in 3D simulation are applied to compute the evolution of the flow matter.

Johnson and Gammie (2006) have performed a series of runs with zero initial vorticity and perturbation wavelengths and have given a very realistic way of the initial vorticity generation.

The simulations of Meheut *et al.* (2012) show that the Rossby vortices can survive for long time scales, if they are sustained by the Rossby Wave Instability in case of permanent mechanism that forms the “overdensity” and launch the instability. They have shown that the Rossby vortices can emerge in a 3D protoplanetary disc and can survive for hundreds of years without migrating.

Although most of the problems concerning the disc’s flow morphology and dynamics are considering as solved and many papers, investigations and works have been devoting to them, there are still unanswered questions.

We aim to study the morphology of the accreting flow and to establish a part of disc’s configuration around the primary (white dwarf) star after the mass transfer through the Lagrangian point being started.

Therefore, when investigating close components, it is necessary to include physical essence of the flow dynamics response to the interaction processes.

By applying numerical calculations on the gas-dynamical flow, we suggest modeling of patterns formation and explanation of supporting physical processes in interacting flows. We present in this paper our 3D numerical calculations of the posted problem, which would be compared to the previously received 2D results. In the section II we briefly introduce the applied methods, equations and conditions of calculations. The results of current study are presented in Section 3.

## 2. METHODS, EQUATIONS AND CONDITIONS

### 2.1. Codes and methods

The complexity of the studied problem and analysis on the corresponding equations in hydrodynamical matter, require applying of numerical codes.

The Maple code is a comprehensive environment for exploring, teaching, and applying mathematics (Heal *et al.* 1998). In addition, Maple 12 is a complete mathematical problem-solving environment that supports a wide variety of mathematical operations such as numerical analysis, symbolic algebra, and graphics.

We chose to insert into the calculations methods, which are implied in the code, known as the Runge-Kutta (implicit part) method. The method treats every step in a sequence of steps in identical manner (Autar and Egwu 2008; Chang *et al.* 1991).

Finite-difference scheme. The basis for the finite-difference method of solution of differential equations is the replacing of derivatives by decrements or difference derivatives.

Alternating direction implicit method (ADI): ADI method belongs to the group of finite difference methods and follows the idea to split the finite difference

equations in two, in relation to the derivatives in coordinates taken implicitly. The system of equations then becomes symmetric and tridiagonal and is usually solved with tridiagonal matrix solver.

The advantage of implicit methods is that they are general in their application and good for partial differential equations, because of their high stability.

We test the equations with the "pdetest" tool, which checks if the solution is correct. To reduce the PDEs to a simpler problem, we applied an "ansatz" tool. Adaptive step-size control is used here (Hairer and Soderling 2005), with the purpose of achieving some predetermined correctness in the solution with minimum computational effort and resources.

Box-multiplying scheme has been suggested, which means that we could perform the calculations in limited regions of the box, defined by the boundary conditions, and then apply it to all disc's area. This could lead to some incorrect solutions, because the behavior of the flow throughout the disc's space is not uniformity. For this reason we should input in these schemes a correction for each of the considering part of the flow and include additional parameters in the calculations. Of course this takes a lot of calculation time and hard math processes. After that, it could be possible to create the model picture of the whole disc's structure. The fast and easy calculation is the advantage of the scheme.

## 2.2. Equations and Conditions

The gas-dynamical system of equations, which has been suggested by many authors (Frank et al. 2002; Graham 2001; Shu 1992), is applied. We consider the influence of viscous processes, gravitational forces, Coriolis force and we add the corresponding terms for viscous non-ideal fluid in the equations. Then our system of equations consists of equation of mass conservation, the Navier-Stokes equations, energy conservation, the equation of state for compressible flow.

$$\begin{aligned} \frac{\partial \rho}{\partial t} + \nabla \cdot (\rho v) &= 0 \\ \frac{\partial v}{\partial t} + v \cdot \nabla v &= -\frac{1}{\rho} \nabla P - \Omega \times (\Omega \times r) - 2\Omega \times v - \nabla \Phi + \nu \nabla^2 v \\ \frac{\partial}{\partial t} \left[ \rho \left( \frac{1}{2} v^2 + \varepsilon + \Phi \right) \right] + \nabla \cdot \left[ \rho v \left( \frac{1}{2} v^2 + h + \Phi \right) - 2\eta \sigma \cdot v \right] &= 0 \\ P &= c_s^2 \rho \end{aligned}$$

Where the basic notations are as follows:  $\rho$  is the mass density of the flow,  $v$  - is the velocity of the flow;  $P$  - is the pressure;  $\nu$  - is the kinematic viscosity;  $\Omega$  - is the angular velocity;  $\Omega \times (\Omega \times r)$  - is the centrifugal acceleration of the centrifugal force; and  $2\Omega \times v$  - is the Coriolis acceleration in the mean of the Coriolis force.  $\Phi$  is the gravitational potential and it depends on the density

distribution inside of the each star's component (Boyarchuk et al. 2002).  $c_s$  is the sound speed.

The expression  $\frac{\partial}{\partial t} \left[ \rho \left( \frac{1}{2} v^2 + \varepsilon + \Phi \right) \right]$  is the total energy density, where the first term on the left denotes the kinetic energy, the second is the internal energy and the third expresses again the full potential of the gravitational fields.

Further  $\left[ \rho v \left( \frac{1}{2} v^2 + h + \Phi \right) \right]$  is the total energy flux, where  $h = \varepsilon + P / \rho$  is the enthalpy,  $\eta$  is the shear (or dynamical) viscosity of the flow, and  $\sigma$  is the rate of shear.

The applied boundary conditions in the calculations are consistent with the studied area of the disc's flow and with a stage of mass transfer. We suggest free boundary conditions at the outer disc edge with constant density:  $\rho_{out} = 10^{-6} \rho_{L_1}$ , where  $\rho_{L_1}$  is the density of the inner Lagrangian point  $\sim L_1$ . In the inner regions, where the mass transfer and the interaction of streams take place, the values of the density could not remain constant.

We set the matter's state of the general flow to be close to the baroclinicity conditions of (Klahr & Bodenheimer 2003):  $\nabla \rho(r, z, \varphi) \times \nabla p(r, z, \varphi) \neq 0$

The boundary conditions of Dirichlet- and Cauchy Type are introduced to control the area of calculations:

$$r_{v(1+n)} = K(x, y, z) - \frac{\partial K}{\partial r_v} \frac{\partial}{\partial t}; \quad r_{v0}(0) = 0 \text{ is the initial radius of the vortex;}$$

$K(x, y, z)$  - the boundary area of equations activity.

It is used the cylindrical coordinates  $(r, \varphi, z)$  frame for the equations and quadratic  $(x, y, z)$  set for the numerical scheme.

We use in the calculations the data for SS Cyg and U Gem that are cataclysmic variables with white dwarf star. For SS Cyg: white dwarf with a mass of  $\sim 0.97 M_{\odot}$ ; Orbital period: 6h 38 min. **U Gem** - hot white dwarf; Mass  $\sim 0.5 - 0.9 M_{\odot}$ . Orbital period: 4 h 11 min.

### 3. RESULTS

For the purpose of this study, the functions of continuous argument are to be replaced by grid functions determined on the difference grid and, as a result, instead of the original differential equation we obtain an algebraic equation.

We divide the calculation domain into finite-difference cells, which are organized in the proposed box-sharing scheme model.

### 3.1. Density distribution

The calculations show that interacting flows via the inconstant tidal mass transfer rate could not remain stable, because of the disturbances in velocity and density. The variability in density and velocity may causes formation of areas with increased density. In the places where the velocity values are close to their minimum, the density starts to increase and it pulls a matter there. Thereafter, this means that the matter from a disc could be pumped out or concentrated within given places, causing the density's dilution in close areas. Based on the research of Bisikalo et al. (2001), we have explained in details in the paper of Boneva and Filipov (2012) how the dense zones in the binary mass transfer area has been formed. Here we make a confirmation of the result, as we run Pp once for in each of orbital periods ( $P_1, P_2, P_3$ ). Steps in moments of rotational period:

$$\sim t_{m0} + 0.25P_p, + 0.57P_p, + 0.78P_p, + 0.92P_p$$

$t_{m0}$  is the time step for zero initial moment;  $P_p$  is the rotational period of the binary corresponds to the values of CV. The numerical series were repeated for  $P_p$ :  $P_{p1} \sim 4h, P_{p2} \sim 5h, P_{p3} \sim 6h$  and fulfilled once  $5.6 P_p$ .

### 3.2. Vortex-like formation

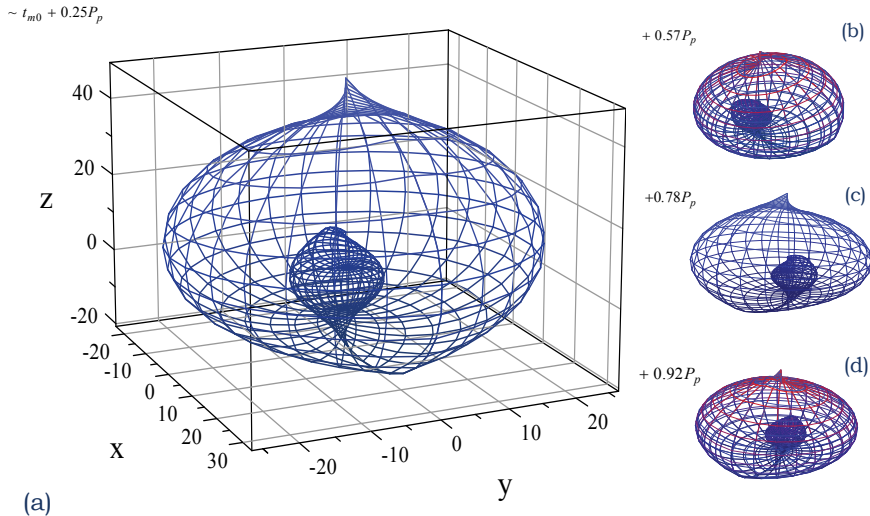


**Figure 1:** 3D view of the thickened zone formation, as a result of disturbances in the stability state, caused by mass transfer in a binary system. The dense pattern's (colored in light blue) behavior during the periods of time is observed in all periods at the image. The mesh grid was taken in a (x, y, z) calculation' frame of coordinates, corresponded to the density distribution in r direction over the time t[d] (Boneva and Filipov 2012).

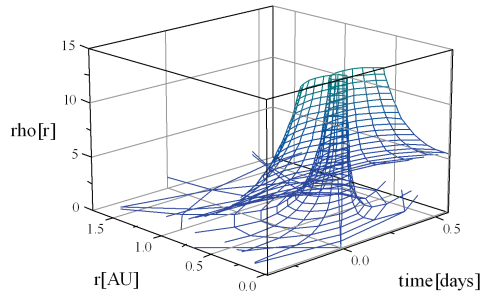


**Figure 2:** Flow density distribution in the area of the thickened zone formation. The image indicates matter accumulation with increased density. Here, the calculation radius  $r$  is in units  $[AU].10^{(-7)}$  and the density maximum value is  $\rho[rho].10^{(-3)}$  (see electronic version).

We received 3D view of the thickened zone formation, as a result of disturbances in the stability state, caused by mass transfer in a binary system. The whole system consecutive phases of rotation can be seen in four images (a),(b),(c),(d) of Fig.1. The dense pattern's behavior during the periods of time is observed in all periods at the image, colored in light blue. The mesh grid was taken to be  $[50, 50, 50]$  in a  $(x, y, z)$  calculation' frame of coordinates. (Boneva and Filipov 2012).

We express the flow's density distribution in time in the area of thickened zone. Fig. 2 depicts the density variation's curves lines with the values concentration, which indicates matter accumulation with increased density. The graphical result is in conformity with the dense pattern formation in Fig. 1.

To compare with the previous results we point to the 2D simulation made by (Boneva and Filipov 2012) and Fig. 3 presents a single vortex formation, which is a part of pattern configuration frame in the covered range of about  $7.687 \times 10^{-8}$  AU to  $6.68 \times 10^{-7}$  AU ( $K(x,y)$  – boundary calculation area). The picture visualizes the final stage of vortex-like development in the flow. The light blue and dark blue colors show the difference in density in the interacting flow layers. The density values are increasing from light to the dark zone.

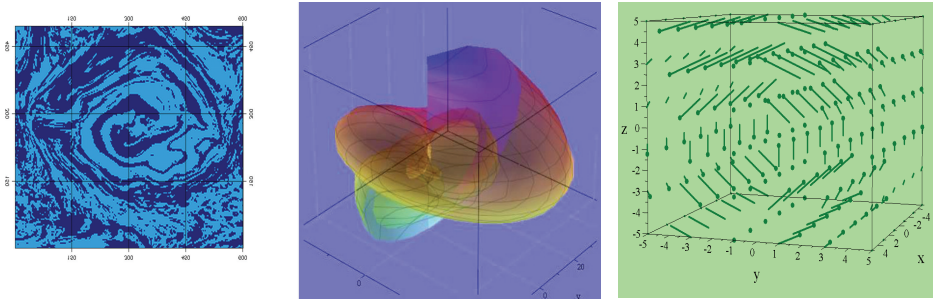


**Figure 3:** Single vortex-like pattern as a result of 2D calculations, with zero initial vorticity, but with initial present of turbulization value different from zero. The boundary calculation area  $K(x,y)$  is covered of about  $7.687 \times 10^{-8} \text{ AU} \div 6.68 \times 10^{-7} \text{ AU}$  (Fig.3a left). 3D result of a single vortex-like structure, with non-zero initial vorticity and function of turbulization is seen at Fig.3b. The boundary calculation area  $K(x,y,z)$  is covered of about  $7.687 \times 10^{-8} \text{ AU} \div 6.68 \times 10^{-7} \text{ AU}$ . The picture shows decomposition in the vortex formation stage. The image in Fig.3c (right) depicts the vector field of vortical formation in a 3D calculation frame.

According to the conditions of the general flow and by applying the simulations we obtain the 3D view of vorticity time evolution in the accreting flow. The box boundary values in this case are:  $K(x, y, z) \in [8 \cdot 10^{-9} \div 7 \cdot 10^{-10} \text{ AU}]$ . The 3D “vortex”-like formation is presented as a patch graphics in the calculating mesh grid (Fig. 3b). Unlike the 2D calculations, here we perform the runs with non-zero initial vorticity and non-zero initial turbulization.

We created the vector field of initial vorticity, seen in Fig. 3c, which gives the basic shape in the calculating box area. In the result, shown in Fig. 3b, an initial deformation in the single vortex-like 3D configuration is observed.

#### 4. CONCLUSION

We presented our study of patterns development in accreting flow around white dwarf stars. The results show that during the mass transfer and interacting processes in the binary, the flow doesn't remain laminar or homogeneous. Comparing to 2D results, 3D calculations show that the dense zone, formed by the disturbances in mass transfer through the binary, keeps its structure, place and stayed stable through the time of rotation. The different situation is observed in the initial behavior of vortex-like configuration, depicted in the box scheme of numerical calculations. We have detected the splitting of the vortex structure wholeness there. It could be seen in the figure.

The vortex, seen in 3D, started to split in small similar-like structures, which would play further role in some new formation around the accretion disc. The accumulation of much of these small dense patterns could lead to throwing of matter out of the disc's space.

Due to the 2D-3D-transition new self organization phenomena probably are observed: as a result from 3D-fluctuations of the velocity gradients the primary density nucleus breaks down into new vorticities whose trajectories draw a tor.

This is only a single result and we could not give any conclusion about the behavior of vortexes in 3D calculations and schemes. New model is needed with related correction, which will give us the construction and view of the whole disc configuration in 3D.

## References

- Autar, K. K., Egwu, E. K.: 2008, Numerical methods with applications, 1st ed., self-publ., ([http://numericalmethods.eng.usf.edu/topics/textbook\\_index.html](http://numericalmethods.eng.usf.edu/topics/textbook_index.html)).
- Barranco, J. A., Marcus, P. S.: 2005, *ApJ*, **623**, 1157.
- Bisikalo, D. V., Boyarchuk, A. A., Kaigorodov, P. V., and Kuznetsov, O. A.: 2003, *Astron. Rep.* **47**, 809.
- Boneva, D. V.: 2010, *BGAJ*, **13**, pp. 3-11, ISSN 1313-2709.
- Boneva, D., Filipov, L.: 2012, Density distribution configuration and development of vortical patterns in accreting close binary star system, submitted to A&A, arXive astro.
- Boyarchuk, A. A., Bisikalo, D. V., Kuznetsov, O. A., Chechetkin, V. M.: 2002, *Adv. in Astron. and Astroph.*, **Vol. 6**, London: Taylor & Francis.
- Chang, M. J., Chow, L. C., Chang, W. S.: 1991, *Numerical Heat transfer*, Part B, **19(1)**, 69-84, ISSN 1040-7790.
- Dan, M., Rosswog, S., Guillochon, J., Ramirez-Ruiz, E.: 2012, *MNRAS*, **Vol. 422**, Issue 3, pp. 2417-2428.
- Frank, J., King, A., Raine, D.: 2002, *Accretion Power in Astrophysics*, 3-rd edition, Cambridge University Press, New York.
- Godon, P., Livio, M.: 1999, *ApJ*, **523**, 350.
- Gokhale, V., Peng, X. M., Frank, J.: 2007, *ApJ*, **655**, 1010.
- Graham, J. R.: 2001, "Astronomy 202: Astrophysical Gas Dynamics", Astronomy Department, UC Berkeley.
- Heal, K. M., Hanse, M. L., Rickard, K. M.: 1998, *Maple V: Learning Guide (for Release 5)*, Springer, New York.
- Hairer, E., Soderling, G.: 2005, *SIAM J. Sci. Comput.*, **Vol. 26**, 6, pp. 1838-1851.
- Johnson, B. M., Gammie, C. F.: 2005, *ApJ*, **635**, 149-156.
- Klahr, H., Bodenheimer, P.: 2003, *ApJ*, **582**, 869-892.
- Lithwick, Y.: 2009, *ApJ*, **693**, 85.
- Marsh, T. R., Nelemans, G., Steeghs, D.: 2004, *MNRAS*, **350**, 113.
- Meheut, H., Keppens, R., Casse, F., Benz, W.: 2012, *A&A*, **542**, A9, arXiveastro: 1204.4390.
- Shen, Y., Stone, J. M., Gardiner, T. A.: 2006, *ApJ*, **653**, 513.
- Shu, F. H.: 1992, *The Physics of Astrophysics, Vol II: Gas Dynamics*.